

Δ DFT predicts inverted singlet-triplet gaps with chemical accuracy at a fraction of the cost of wavefunction-based approaches

Lukas Kunze,^a Thomas Froitzheim,^a Andreas Hansen,^a Stefan Grimme,^a and Jan-Michael Mewes^{a,b*}

^a*Mulliken Center for Theoretical Chemistry, Clausius Institute for Physical and Theoretical Chemistry, Rheinische Friedrich-Wilhelms Universität Bonn, Berlingstraße 4, 53115 Bonn, Germany and*

^b*beeOLED GmbH, Niedersedlitzer Str. 75c, 01257 Dresden, Germany*

(Dated: June 2, 2024)

Efficient OLEDs need to quickly convert singlet and triplet excitons into photons. Molecules with an inverted singlet-triplet energy gap (INVEST) are promising candidates for this task. However, typical INVEST molecules have drawbacks like too low oscillator strengths and excitation energies. High-throughput screening could identify suitable INVEST molecules, but existing methods are problematic: The workhorse method TD-DFT can't reproduce gap inversion, while wavefunction-based methods are too slow. This study proposes a state-specific method based on unrestricted Kohn-Sham DFT with common hybrid functionals. Tuned on the new INVEST15 benchmark set, this method achieves an error of less than 1 kcal/mol, which is traced back to error cancellation between spin contamination and dynamic correlation. Applied to the larger and structurally diverse NAH159 set in a black-box fashion, the method maintains a small error (1.2 kcal/mol) and accurately predicts gap signs in 83% of cases, confirming its robustness and suitability for screening workflows.

Introduction — Molecules with an inverted singlet-triplet energy gap (INVEST) have become a hot research topic as they would enable highly efficient emitters for organic light-emitting diodes (OLEDs).^{1–12} In OLEDs, excited states (or excitons) are created by recombining electrons and holes.¹³ According to Fermi-Dirac spin statistics, the ratio of singlet to triplet excited states generated via recombination is 1:3. Hence, any purely fluorescent emitter's internal quantum efficiency (IQE) is limited to 25%. Overcoming this limitation, modern emitters can thus harvest singlet and triplet excited states, either via phosphorescence in so-called PhOLEDs, or by upcycling triplets via reverse intersystem crossing (rISC) into light-emitting singlet excited states. The latter phenomenon is termed thermally activated delayed fluorescence (TADF) and has been intensively studied.^{11,14–20}

A key property of TADF emitters is a small energy gap ΔE_{ST} between S_1 and T_1 states^{17,18}

$$\Delta E_{ST} = E_{S_1} - E_{T_1}, \quad (1)$$

which is necessary to enable efficient triplet up-conversion. This is typically achieved by introducing a large spatial separation between the highest occupied molecular orbital (HOMO), located on a donor, and the lowest unoccupied molecular orbital (LUMO), located on the acceptor. A problem of this straightforward design is that small overlap also leads to vanishing spin-orbit coupling (SOC) and oscillator strength

(f_{osc}) between the states of interest,²¹ which negatively impacts (r)ISC and radiative decay rates. Additionally, such classical D-A-type TADF emitters exhibit the broad emission peaks characteristic of long-range charge-transfer (LRCT) states, which is the opposite of the desired sharp (color-pure) emission.²²

In these regards, the discovery of multi-resonance TADF (MR-TADF) emitters changed the picture.²² In contrast to the D-A architecture, MR emitters achieve a small electron-hole overlap by distributing the HOMO and the LUMO on alternating positions of an aromatic π -system.²³ Although this does not reduce electron-hole overlap as much as in D-A emitters and, in turn, leads to larger singlet-triplet gaps, other photophysical properties of MR-TADF emitter are more favorable: The emission spectrum of MR-emitters is sharp and thus color pure with high oscillator strength.^{22,24} Because of this and further desirable properties, DABNA and its derivatives are used as fluorescent blue emitters in mass-produced OLED displays.²⁵

Regarding their molecular and electronic structure, MR-type emitters can be regarded as a bridging element between classical D-A-type TADF emitters and INVEST-type emitters (cf. Figure 1). Analogous to MR-TADF emitters, INVEST emitters give up the spatial separation between donor and acceptor in favor of a strategy with alternating orbital lobes. The perhaps most prototypical examples for INVEST systems are cycl[3.3.3]azine and its derivatives, of which heptazine, a nitrogen-doped variant, has been experimentally shown to have properties that confirm an inverted ΔE_{ST} .¹¹ In a two-dimensional polymeric variant of heptazine, amorphous carbon nitride, Actis *et al.* observed

* Correspondence email address: janmewes@janmewes.de

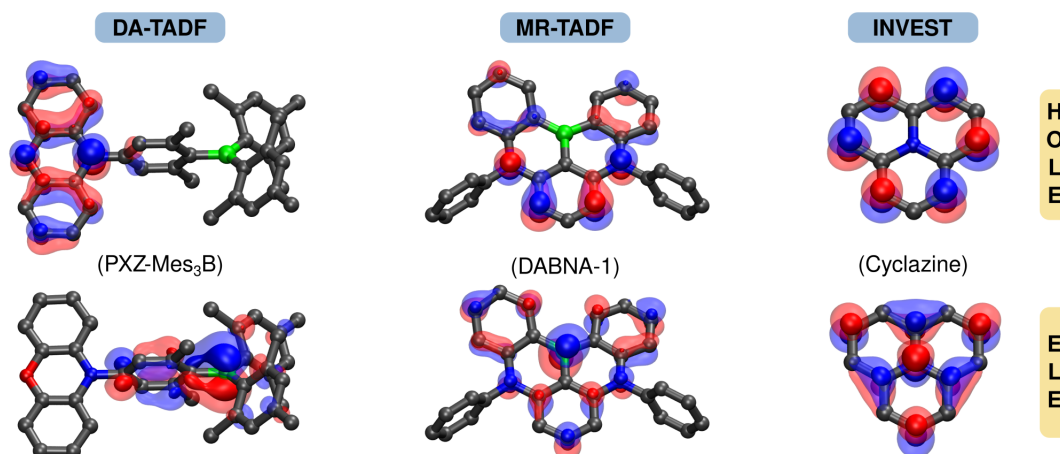


Figure 1. Hole and electron molecular orbitals (MO) from a Δ UKS calculation with the FX175- ω PBE functional for a donor-acceptor type TADF emitter (DA-TADF), a multi-resonant TADF emitter (MR-TADF) and an inverted singlet-triplet gap molecule (INVEST), isovalues of 0.08 Bohr^{-3} and 0.04 Bohr^{-3} were used for the inner (solid) and outer (transparent) isosurface respectively.

in steady-state optical spectroscopy an inversion of singlet and triplet excitons by roughly 0.2 eV.²⁶ During the final stages of the preparation of this manuscript, another study reported the experimental determination of INVEST for a pentaazaphenylene (molecule #4 in our INVEST15 benchmark introduced below) derivative.²⁷

The special structure of these triangulene-like systems leads to an inversion of the singlet-triplet gap, meaning that in violation of Hund's rule, the S_1 is energetically lower than T_1 . As a result, rISC changes from an uphill conversion process of triplet to singlet excitons in DA- and MR-TADF emitters to a downhill process in INVEST systems, which should translate into more efficient triplet harvesting and lower efficiency roll-off at high brightness. However, the inverted gap comes at a cost: The electronic structure that gives rise to an inverted gap causes poor photophysical properties, such as low oscillator strengths. Therefore, it is one of the most essential tasks to find INVEST emitters that combine an inverted gap with favorable emission properties.⁷ Unfortunately, systematic high-throughput screenings are hindered by the reality that MR-TADF and INVEST emitters are only poorly described by time-dependent density functional theory (TD-DFT²⁸), which is by far the most prominent and efficient workhorse in materials science. More specifically, it seems that the short-range charge-transfer (SRCT) states that emerge from the MR-TADF and INVEST scaffolds are poorly described by TD-DFT and its Tamm-Dancoff-approximated variant (TDA-DFT²⁹), which predicts systematically too high singlet excitation energies and qualitatively wrong ΔE_{ST} (*vide infra*). In contrast to the shortcomings of TD-DFT with the description of the LRCT states and their dielectric

embedding in classical TADF emitters,^{30,31} the issues TD-DFT has with SRCT states can not be mitigated by using modern functionals and more complete solvation models, but are inherent to the underlying theory.

Hall and coworkers tested a variety of hybrid and range-separated hybrid functionals with different amounts of Fock exchange (FX) and range-separation parameters for MR-TADF emitters.³² They attributed the imbalanced description of S_1 and T_1 with errors in ΔE_{ST} of up to 1.0 eV to the absence of doubly-excited determinants in TD(A)-DFT, which affects the excited singlet states much more than the triplets.³³ In their recent study, which employed wavefunction-based correlated methods in addition to TD-DFT, Drwal *et al.* pointed out an implicit connection between doubly excited determinants and spin-polarization effects, which specifically stabilize the S_1 state out of a pair of singlet and triplet excited states involving the same molecular orbitals.³⁴ The spin-polarisation balances the increasing electron-hole overlap and dynamical correlation, which together destabilize the S_1 relative to the T_1 state. Further works confirm the hypothesis that doubly excited determinants exert a large and selective influence on the energy of the singlet excited state.^{1,5,35-37} This different impact of doubly excited configurations on singlet and triplet states explains why in wavefunction theory, highly correlated methods including at least up to triple substitutions are required for a balanced description of INVEST molecules (*vide infra*).

The conclusion derived by most authors is that computationally demanding correlated wavefunction-based approaches are necessary to describe the inversion of S_1 relative to T_1 . For example, linear-response second-order approximate coupled cluster singles and

doubles (LR-CC2³⁸), second-order algebraic diagrammatic construction (ADC(2)^{39,40}) and their spin-scaled variants^{41,42} (SCS-CC2, SCS-ADC(2)), as well as state-averaged complete-active space self-consistent-field-based approaches (SA-CASSCF⁴³, SC-NEVPT2⁴⁴, and CASPT2^{45,46}) are often used to study INVEST emitters because they include these effects at a manageable computational cost.^{6,7,36,37,47} However, in face of the importance of doubly excited determinants, it is surprising that second-order methods like CC2 or ADC(2) perform quite well for INVEST cases.

Further studies seek a more complete description that includes even higher-order correlation effects using state-specific coupled cluster with up to triple substitutions. Notably, Dreuw *et al.* reported a decrease of the inverted gaps or even positive ΔE_{ST} -values for prototypical INVEST emitters when they systematically converged the level of theory by increasing basis set size and correlation treatment, questioning the existence of inverted ST-gaps.⁴⁸ Specifically, they used a state-specific coupled cluster approach with unrestricted Hartree-Fock reference wavefunctions [termed $\Delta\text{CCSD(T)}@HF^{49}$], as well as the ADC method of up to third order.³⁴ Meanwhile, a minimal CASSCF(2,2) reference in Mukherjee’s MRCC-formalism [Mk-MR-CCSD(T)@CAS(2,2)^{50,51}] used by Drwal *et al.* tends to yield more negative gaps.³⁴

Having established that various high-level single- and multi-reference methods agree with each other and can thus be considered converged, Loos and coworkers recently demonstrated that also the relatively efficient LR-CC2 and ADC(2) methods agree surprisingly well with EOM-CC3⁵² and EOM-CCSDT^{53,47}. Although this agreement has been traced back to error-cancellation effects, it means that INVEST systems can be modeled with widely available and relatively efficient (compared to MR-CC) ADC(2) or LR-CC2 methods. However, even these calculations take hours for typical INVEST molecules with converged, i.e., augmented triple-zeta basis sets, rendering them too costly to execute automatic screening workflows with thousands or even millions of molecules.

Addressing this major challenge, a recent work by Jorner and coworkers has presented a special-purpose semi-empirical quantum-chemical method focusing on the π -electrons (PPP theory).⁵⁴ Exploiting dynamic spin-polarization to recover the gap inversion, their PPP method shows a promising correlation with ADC(2) calculations after introducing several correction terms. While clear advantages of the method are its speed (less than a second per molecule) and robustness against technical issues (> 99.9% convergence in a test application), downsides are that it requires specialized software and, moreover, a clear separation between σ and π -electrons, which excludes some functional groups.

This study presents a less approximate and thus

slightly more costly (minutes per molecule) approach to predict ΔE_{ST} and absolute state energies accurately and reliably with standard quantum-chemical software packages. To this end, we use state-specific unrestricted Kohn-Sham (UKS) DFT, targeting the respective singlet (and triplet) states by converging a non-Aufbau initial guess (typically HOMO-LUMO) with the help of the initial maximum-overlap method (IMOM),^{55,56}. Since this state-specific approach treats each excited state separately, orbital relaxation effects for any excitation are explicitly included in the description at a much lower cost than comparably accurate response methods. In addition to UKS, we test the closely related restricted open-shell Kohn-Sham (ROKS)^{57–59} method, which, in contrast to UKS, provides a correct open-shell singlet with $\langle S^2 \rangle = 0$. To illustrate the approach, we explore the influence of the functional, focusing on the type and amount of exact exchange mixing, which has by far the largest impact on the computed gaps. The method is tested in comparison to high-level reference values collected from the literature for a set of 15 INVEST molecules sharing the prominent cyclazine motif. We then rationalize the reliability of the ΔUKS approach by comparing it to state-specific post-SCF correlation methods. Finally, we apply the approach to a larger and structurally diverse validation set, introducing a simple trick to eliminate issues relating to the state-specific nature of the approach, thereby increasing its robustness as is required for an application in high-throughput screenings.

Benchmark Set and Reference Values — Based on recently published high-level calculations, we compiled the benchmark set INVEST15, which includes 15 INVEST emitters based on the cyclazine-scaffold, featuring various doping patterns and heteroatoms. 10 of the 15 molecules were taken from a recent work of Loos *et al.*⁴⁷, in which they provided theoretical best estimates (TBE) using the most accurate methods available for those types of molecules, namely EOM-CC3 and EOM-CCSDT (with incremental corrections up to augmented triple zeta basis set level). Five additional literature-known INVEST emitters, namely 3³⁶ and 10, 11, 14 and 15⁷ originating from two papers of Ricci *et al.* were picked to diversify our test set and doping patterns. System 15 was added as a sanity check to have at least one positive ΔE_{ST} . B97-3c optimized ground-state geometries were used for all INVEST15 systems, which showed fairly small root-mean-square deviations (RMSDs) compared to CCSD(T)/cc-pVTZ geometries (taken from Loos’ benchmark set) typically around 0.005 Å.

The INVEST15 will serve as our test set for different functionals, basis sets, etc., while a second benchmark set by Garner *et al.*⁶⁰ will serve as our validation set (see Figure 2). The second set consists of substituted variants derived from systems 1, 4, and 6 of our INVEST15

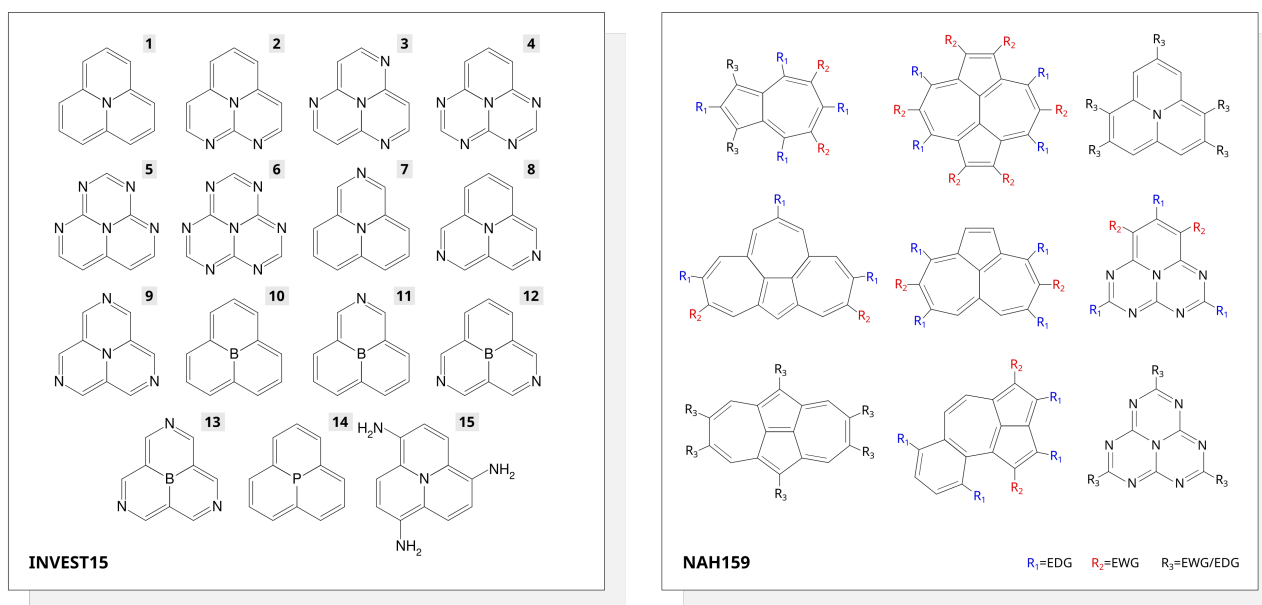


Figure 2. INVEST15 benchmark set, a selection of 15 cyclazine derivatives, differing in doping pattern and doping atoms and NAH159, a selection of substituted cyclazine derivatives and non-alternant hydrocarbons, only an excerpt is shown with positions of electron-donating (EDG) and electron-withdrawing groups (EWG) colored blue and red, respectively.

benchmark set, as well as substituted variants of non-alternant hydrocarbons not part of NVEST15. In total, the validation set comprises 159 distinct systems, which we will refer to as NAH159 for simplicity.

In light of the fragmented reference data, we perform extensive tests of both state-specific coupled cluster approaches (namely Δ CCSD(T) and Mk-MR-CCSD(T)), as well as LR-CC2. We find that Mk-MR-CCSD(T) based on a reference wavefunction with only the two singly excited determinants (denoted $\langle \uparrow\downarrow | \pm \langle \downarrow\uparrow |$)^{61,62} and LR-CC2 agree very closely with the TBE of Loos and coworkers (see Supporting Information for details). Therefore, we choose LR-CC2/aug-cc-pVTZ as the secondary reference method to provide consistent reference data for the larger NAH159 set.

To further investigate and rationalize the performance of the Δ UKS/PBE0 approach, we use the unrestricted Kohn-Sham wavefunction as a basis for Δ CCSD and Δ CCSD(T) calculations with Q-Chem,^{49,63} and compare the results to those obtained with a canonical UHF reference similar to Dreuw and coworkers.⁴⁸ Recognizing the importance of spin-contamination (which refers to the deviation from the $\langle S^2 \rangle$ expectation value of the wavefunction, e.g., 1.2 instead of 1.0) and spin-adaptation (by which we refer to changing the formally wrong $\langle S^2 \rangle$ of a single-reference open-shell singlet of 1 to its correct value 0), we explored the impact of the Yamaguchi spin-correction based on the $\langle S^2 \rangle$ expectation value from CCSD.⁶⁴ The underlying reason is that the singlet state obtained with UKS is usually a 50:50

mixture of singlet and triplet state exhibiting an ideal $\langle S^2 \rangle = 1.00$. This is a direct result of the UKS approach using only a single determinant.

Finally, to eliminate any spin-related issues in wavefunction-based Δ approaches, we also considered a multi-reference level of theory with exactly two reference determinants. Namely, we calculated state-specific Mukherjee multi-reference coupled cluster with perturbative triple excitations [Mk-MR-CCSD(T)] on a reference wavefunction consisting of the required two singly excited determinants for proper spin-adaptation.⁶⁵ This level of theory is for a strict two-determinant state,^{61,62,66} at least formally, the most highly correlated method used in this work, and presumably even superior to EOM-CCSDT of Loos and coworkers since excited states are targeted directly and no substitutions have to be spent to generate the excited states from the ground-state reference (see also SI).

Computational Details and Workflow — Several different programs were used throughout this study, including the Q-Chem program version 5.4.2⁶⁷ (for all Δ UKS, Δ ROKS, Δ CC, and TDA-DFT^{28,29} excited-state calculations), the ORCA program version 5.0.4⁶⁸ (for all DFT^{69,70} ground-state geometry optimizations), the mrcc program⁷¹ (for all single-reference correlated WFT calculations, mainly LR-CC2³⁸), the NWChem program version 7.2.2^{72,73} with the Tensor Contraction Engine⁷⁴ (for all multi-reference correlated WFT calculations), the DALTON program version 2020.1^{75,76}

(for CC3⁵² calculations). The ground-state geometry optimizations were carried out with the B97-3c⁷⁷ composite method. Symmetry constraints (C_{3h}) were enforced only for system 15, to be consistent with existing literature references. Comprehensive conformer searches for the ground-state geometries were omitted since the investigated molecules are rigid and planar, having only one self-evident low-energy structure. For all excited-state energy calculations for the INVEST15 (Δ UKS, Δ ROKS, Δ CC, Mk-MR-CCSD(T), LR-CC2, and LR-CC3), the B97-3c optimized ground-state geometries were used. In contrast to D-A-TADF emitters, the influence of the solvent is negligible (<0.02 eV for the best-performing Δ UKS/PBE0 approach in toluene, see Figure S5). Therefore, only gas phase calculations were considered. Δ UKS and Δ ROKS methods were used in combination with the large Ahlrich's def2-TZVPP^{78,79} basis set. All post-SCF Δ WFT calculations are conducted using Dunning-type basis sets up to cc-pVTZ.^{80,81} The Mk-MR-CCSD(T) calculations adhere to a similar procedure as outlined by Drwal *et al.*³⁴ with a def2-TZVP basis set in the NWChem program (see SI for further details).^{72,73} LR-CC2 and LR-CC3 calculations employ the aug-cc-pVTZ⁸² and cc-pVDZ basis sets, respectively. The Δ UKS approach was used in conjunction with the initial maximum-overlap method (IMOM)^{55,56} to prevent variational collapse to the ground-state. For calculations on the validation set of 159 molecules, geometries optimized at the ω B97X-D⁸³/def2-TZVP level were taken from a recent publication by Garner *et al.*⁶⁰ As the reference for the NAH159, vertical singlet-triplet energy gaps were calculated at the LR-CC2^{38,84}/aug-cc-pVTZ level, to be consistent with the references in the INVEST15 set. Δ UKS calculations for vertical singlet-triplet gaps of the validation set were carried out in the def2-SVP basis set with the PBE0 functional to simulate a screening application.

Results and Discussion — We begin our investigation by exploring the effect of the DFT functional on the Δ UKS approach, including results obtained with TDA-DFT and ROKS to complete the picture. Since the most important parameter in the DFT functional turned out to be the amount of Fock exchange (FX), we selected a hierarchy of PBE-based DFAs with increasing admixture of FX, namely PBE,⁸⁵ PBE0,^{86,87} PBE38,⁸⁸ PBE50,⁸⁹ and LC- ω PBE,⁹⁰ as well as the tuned RSH FX175- ω PBE with a ω value of 0.175 that was found to be most accurate for CT states of TADF and MR-TADF emitters in previous work.^{30,91}

First, let us discuss the TDA-DFT results for the vertical ΔE_{ST} gaps shown in Figure 3a). As expected, TDA-DFT yields positive ΔE_{ST} for all 15 molecules, irrespective of the amount and type of FX admixture. This can be rationalized by the lack of doubly excited determinants in TDA-/TD-DFT, which causes the re-

spective S_1 state to be too high in energy.⁹²⁻⁹⁴ Only for molecule 15, which has a positive singlet-triplet gap, TDA-DFT with the PBE functional agrees reasonably well with the reference. Generally, there is a clear systematic trend to larger gaps with an increasing amount of FX, which is the same for DA-type TADF emitters.³⁰ Moreover, despite this failure of TDA-DFT to reproduce absolute gaps, the relative trends between the INVEST15 systems are recovered rather well. These trends are also reflected in the Bessel-corrected standard deviation (SD) for TDA-PBE0 (see I), which is just 0.075 eV, compared to 0.381 eV for the mean absolute deviation (MAD), pointing at the systematic error of TDA. To illustrate this, we have added a dashed line with the TDA-PBE0 results down-shifted by -0.4 eV (MD vs TBE) in Figure 3a). Inspection shows a reasonable agreement with the high-level references, indicating that the effect of double excitations on the singlet energy is rather consistent. However, one should be clear that this is based on error cancellation effects that are enabled by the structural similarity of the molecules in the INVEST15 set.

Therefore, let us move to the state-specific Δ SCF approaches, namely Δ UKS and Δ ROKS, which do not have the same issues with doubly excited determinants. Despite its state-specific nature and its principle ability to deal with double excited states, Δ ROKS (Figure 3b) is not more accurate than TDA-DFT, which is in stark contrast to a recent benchmark for D-A-type and MR-TADF emitters.⁹¹ Similar to TDA-DFT, Δ ROKS systematically overestimates gap sizes to an extent where it only provides positive gaps. Moreover, in contrast to TDA-DFT, relative trends between the systems are worse, as shown by the SD of Δ ROKS/PBE0 of 0.202 eV. The issue appears to be the lacking doubly-excited LUMO² singlet configuration (D_{CS} -type double excitation in Ref.⁹⁵) in the ROKS approach, which is responsible for the spin-polarisation (the respective triplet-reference required for ROKS spin-purification does not exist). Hence, we conclude that Δ ROKS is unsuitable for application to INVEST systems, and presumably even more generally for D_{CS} -type doubly excited states.

In contrast to ROKS, the Δ UKS results shown in Figure 3b) all exhibit a trend similar to the various high-level reference methods, while the amount of Fock exchange appears to scale the gaps (the more FX, the more negative the gaps). With the RSH LC- ω PBE with a range-separation parameter of 0.175 (termed FX175- ω PBE, established to be optimal for TADF emitters in previous work)⁹¹, and even with the common admixture of 25% of FX as in PBE0,⁹⁶ UKS provides exceptional agreement and virtually lies on top of the high-level references for all but two cases, namely system 3 (lacking uptick), and system 15 (too small positive gap). Even more FX, in PBE38, PBE50, or LC- ω PBE with the de-

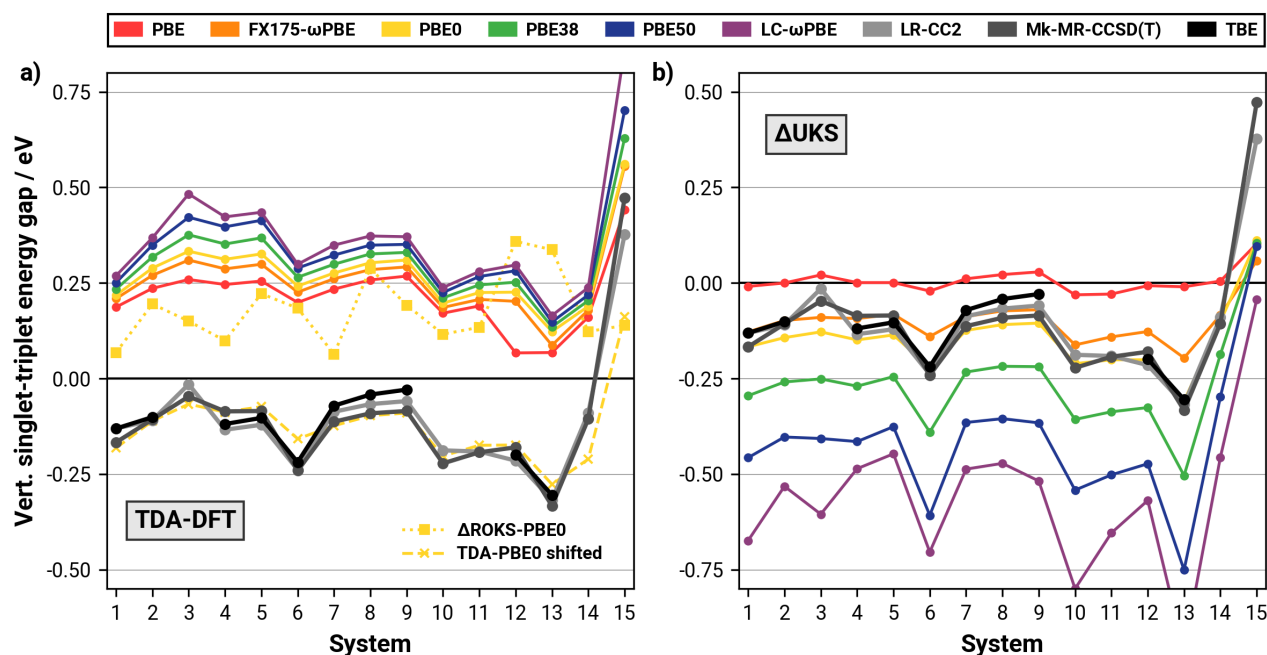


Figure 3. Vertical singlet-triplet energy gap for investigated molecules calculated by **a)** TDA-DFT, ROKS/PBE0 and **b)** Δ UKS for various functionals of the PBE-family with different amounts of FX (increases from red to blue), all values in eV. The TBE is obtained from CC3/aug-cc-pVTZ + [CCSDT/6-31+G(d) - CC3/6-31+G(d)] for S_1 and CC3/aug-cc-pVDZ + [CCSD/aug-cc-pVTZ - CCSD/aug-cc-pVDZ] for T_1 as defined by Loos *et al.*⁴⁷ All TD-DFT and Δ DFT calculations use the def2-TZVPP basis set.

fault range-separation parameter of 0.45, provides systematically too negative ST-gaps, whereas too little or no FX as in the pure PBE functional provides too positive gaps.

Interestingly, modern pure functionals like the meta-GGA r^2 SCAN⁹⁷ (and to some extent also B97M-V)⁹⁸ remedy the shortcomings of PBE. r^2 SCAN performs almost equal to UKS/PBE0 (MAD against CC2 is 0.053 eV vs 0.046 eV for PBE0, cf. Table I) and becomes better if the outlier (*vide infra*) is removed (MAD 0.037 eV vs 0.049 eV for PBE0, cf. Figure S3 in the SI) albeit these differences are only borderline significant. However, there is also one issue, namely a systematic underestimation of nitrogen $n\pi^*$ states, which can artificially become S_1 or T_1 , causing outliers, e.g., for molecule 13 (here the actual $\pi\pi^*$ states are S_2 and T_3 , whose gap is spot-on (cf. Figure S3)). Irrespective of those outliers, it appears that the exchange-functional of r^2 SCAN mimics some properties of non-local FX, which has previously been reported in the context of self-interaction error.⁹⁶ Moreover, since pure functionals enable a substantial speedup over hybrids due to full exploitation of density-fitting,⁹⁶ they can offer an even faster screening for INVEST if $n\pi^*$ states could be automatically identified. We are currently exploring this possibility.

Statistical metrics for Δ UKS, Δ ROKS, and TDA-DFT for the best-performing functionals PBE0 and FX175- ω PBE are given in Table I. The best-performing

Table I. Statistical error metrics (formulas in the SI) for various tested methods against TBE and LR-CC2/aug-cc-pVTZ reference data, DFT calculations use the def2-TZVPP basis set, Mk-MR-CCSD(T) calculations use the def2-TZVP basis set, all values in eV.

Method	MD	MAD	RMSD	SD	AMAX
against TBE					
(excl. 3, 10, 11, 14, 15)					
CC2	-0.016	0.016	0.018	0.009	0.030
Mk-MR-CCSD(T)	-0.017	0.031	0.034	0.031	0.056
Δ PBE0	-0.035	0.035	0.043	0.026	0.076
Δ FX175- ω PBE	0.023	0.041	0.053	0.051	0.114
Δr^2 SCAN	0.007	0.052	0.088	0.093	0.263
against CC2					
Δ PBE0	-0.041	0.046	0.079	0.070	0.266
Δ FX175- ω PBE	0.005	0.060	0.099	0.103	0.319
Δr^2 SCAN	-0.007	0.053	0.100	0.103	0.276
Δ ROKS/PBE0	0.284	0.315	0.344	0.202	0.655
TDA-PBE0	0.381	0.381	0.388	0.075	0.481
TDA-PBE0(-0.4 eV)	-0.019	0.055	0.075	0.075	0.216

method, Δ UKS with PBE0, shows a MAD of only

0.035 eV against the TBE, achieving chemically accurate (better than 1 kcal/mol \approx 0.043 eV) results against a high-level WFT method. The non-zero MD of PBE0 provided in Table I suggests that a slightly smaller fraction of FX of around 20% would render the MD closer to zero, further improving the MAD. However, it is questionable if such small changes for a limited number of molecules transfer to the bigger picture. The more modern tuned RSH FX175- ω PBE performs comparably well with an MAD and RMSD of 0.041 eV and 0.053 eV. Finally, we want to point out that the accuracy of the approach is retained even with a smaller basis set, as evident from the def2-SVP to def2-TZVPP RMSDs for PBE0 of only 0.016 eV (see SI for details). This enables much more efficient calculations, as the walltime with def2-SVP is about 15-18 times shorter than with def2-TZVPP.

Another interesting observation is that system 15, the only one with a positive gap, steps out of line. Here the different functionals become much more similar, indicating that the strong dependence on the amount of FX vanishes for molecules with positive gaps. This is in line with our earlier study on the singlet-triplet gaps of TADF emitters, where Δ UKS and Δ ROKS were much less sensitive to the amount of FX in the DFA than TD-DFT.⁹¹ At the same time, this system shows the largest deviation between the best-performing Δ UKS approaches and the high-level references of around 0.3 eV, almost ten times the MAD.

Table II. Singlet and triplet excitation energies (EEs) of the LR-CC2 reference and deviations for the PBE0 functional using Δ UKS and TDA-DFT for the INVEST15 benchmark set, all values in eV.

mol.#	S_1			T_1		
	CC2	$\Delta_{\text{CC2}}^{S_1}$	TDA	CC2	$\Delta_{\text{CC2}}^{T_1}$	TDA
1	1.05	-0.15	0.25	1.18	-0.11	-0.10
2	1.61	-0.17	0.26	1.71	-0.14	-0.13
3	2.12	-0.27	0.16	2.14	-0.16	-0.19
4	2.21	-0.20	0.25	2.35	-0.19	-0.20
5	2.16	-0.19	0.27	2.28	-0.17	-0.18
6	2.75	-0.17	0.28	2.98	-0.19	-0.20
7	0.90	-0.16	0.26	0.99	-0.13	-0.11
8	0.76	-0.18	0.26	0.83	-0.14	-0.11
9	0.62	-0.19	0.26	0.68	-0.14	-0.11
10	0.85	-0.17	0.23	1.04	-0.15	-0.16
11	1.08	-0.17	0.25	1.27	-0.16	-0.17
12	1.32	-0.16	0.26	1.53	-0.17	-0.18
13	1.57	-0.13	0.28	1.89	-0.14	-0.16
14	1.27	-0.13	0.21	1.36	-0.12	-0.06
15	1.56	-0.50	-0.08	1.18	-0.23	-0.27

After careful analysis of the gaps, let us now briefly consider the excitation energies of the S_1 and T_1 , which are collected for the high-level references and the PBE0-

based DFT methods in Table II (for all methods, see Figure S1 in the SI). Inspection shows highly systematic deviations between S_1 and T_1 excitation energies of the LR-CC2 reference and Δ UKS/PBE0, which leads to the previously established agreement for the gaps. For TDA-PBE0, the triplet energies are similar, whereas the deviation for the singlets is larger (by 0.4 eV) and of opposing sign. This can be rationalized by the aforementioned lack of doubly-excited determinants (and spin-polarization). Further analysis of the UKS results shows that the deviations strongly depend on the amount of FX (see SI), where the deviations for S_1 and T_1 cancel each other at around 25%. The relation between spin-contamination and excitation energy is also evident from Figure 4b), which displays the $\langle S^2 \rangle$ expectation values of the S_1 excited states for the INVEST15 set (the respective data for the spin-adapted T_1 can be found in the SI): While intermediate amounts of FX found in FX175- ω PBE and PBE0 lead to some spin-contamination of S_1 with $\langle S^2 \rangle = 1.15$, going to pure HF leads to a highly contaminated state with $\langle S^2 \rangle > 2$. Dynamic spin-polarisation was previously identified as the driving mechanism for the singlet-triplet gap inversion,³⁴ and may explain why FX in combination with PBE is essential for the excellent performance of PBE0. While this appears to be the working mechanism of hybrid functionals, it does not apply to semi-local functionals. However, although no FX is admixed in the well-performing r²SCAN functional, the spin-contamination of the singlet state is nearly identical to that of PBE0 (see Figure S4 in SI), suggesting that a similar error-cancellation mechanism is at work here.

Lastly, we want to point out that similar error-cancellation effects have been reported in a study on doublet excited states in structurally similar triangular molecules.⁹⁹ In their careful analysis of a comparison between single-reference (UKS/UHF, ROHF) and multi-reference methods, the authors demonstrated that spin-contamination in a UKS/UHF reference leads to negative contributions to the spin density, mimicking an electron correlation effect in the MR reference calculation. In further analogy, the error cancellation worked best with small amounts of FX admixture for the spin-unrestricted wavefunction, but not for the spin-restricted ROHF. Hence, we speculate that the presence of this spin-polarization (*vide infra*) mechanism explains the robustness of this error cancellation.

Having explored the effect of mixing DFT and FX in unrestricted Kohn-Sham calculations, we now systematically investigate the treatment of dynamic correlation beyond the Kohn-Sham correlation functional. For this purpose, we employ a set of increasingly sophisticated post-SCF correlation methods – namely CCSD and CCSD(T) – based on the unrestricted open-shell singlet and triplet reference wavefunctions from the

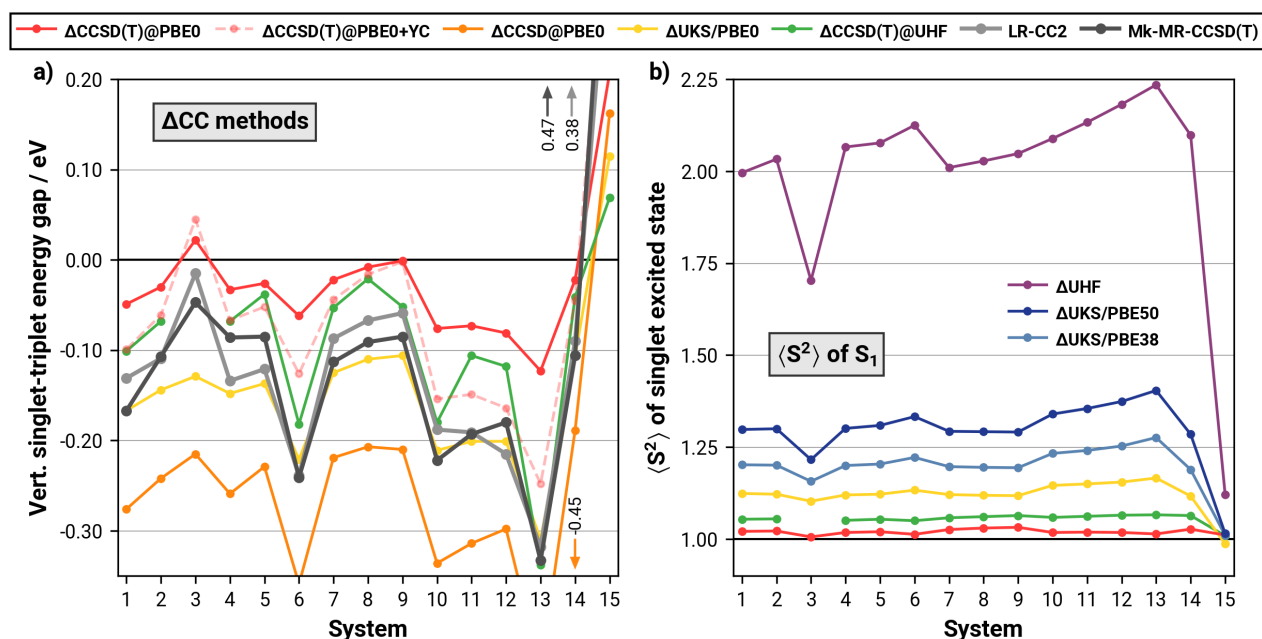


Figure 4. A) Δ WFT (CCSD and CCSD(T)) results in cc-pVTZ basis for investigated molecules compared to Δ UKS/PBE0 and excitation-based WFT (LR-CC2, TBE*), all values in eV. Basis set effects are investigated in the SI. B) $\langle S^2 \rangle$ expectation values for different SCF and post-SCF methods. The respective plots for the triplet can be found in the SI.

Δ UKS/PBE0 calculations as well as on a (highly spin-contaminated) Hartree-Fock reference. Inspection of Figure 4a shows that while CCSD generally provides much too negative gaps (orange line), the "gold standard" CCSD(T) (red and green lines) provides too positive gaps. We argue that such a large effect of the (T) correction indicates that dynamical correlation strongly differs between the singlet and triplet states, explaining why explicitly including triples is required for a balanced description of INVEST. Moreover, the resulting gaps depend strongly (by up to 0.15 eV or ≈ 3 kcal/mol) on the reference wavefunction (UHF vs PBE0). Analysis shows that this behavior is again related to the $\langle S^2 \rangle$ of the reference and CCSD wavefunctions depicted in Figure 4b. With UHF (red line) both the open-shell S_1 and T_1 states suffer from substantial artificial spin-symmetry breaking ($\langle S^2 \rangle_{S_1} = 1.1 - 2.2$ and $\langle S^2 \rangle_{T_1} = 2.4 - 2.8$), while for Δ UKS/PBE0 (orange line) only the S_1 is weakly spin-polarized ($\langle S^2 \rangle_{S_1} = 1.0 - 1.1$ and $\langle S^2 \rangle_{T_1} = 2.0$). CCSD repairs this spin-contamination of both HF and PBE0 orbitals, as evident from Figure 4b (green and red lines). However, since UHF starts much further away from the ideal value, the resulting $\langle S^2 \rangle$ values are distinctly closer to the ideal of 1.0 for a spin-broken S_1 with PBE0 orbitals than with HF orbitals (note that T_1 is generally much less contaminated and less interesting for this discussion). In line with our interpretation of the FX admixture to DFT, the removal

of spin-polarization leads to a reduction in the magnitude of the inverted gaps compared to the reference wavefunction. Accordingly, the small remaining differences in $\langle S^2 \rangle$ values for Δ CCSD(T)@HF (green line) and Δ CCSD(T)@PBE0 (red line) explain the remaining differences in ΔE_{ST} . We attribute this difference to the reduced flexibility in Δ CCSD(T)@HF to recover dynamic correlation when dealing with spin-contaminated references, which has recently been reported for in transition-metal complexes.¹⁰⁰ Accordingly, and in line with Drwal and Dreuw,^{34,48} we observe that including more dynamic correlation in coupled-cluster calculations diminishes the magnitude of inverted gaps, which becomes evident when comparing Δ CCSD (orange line in Figure 4a) to Δ CCSD(T).

Nevertheless, even the virtually spin-pure Δ CCSD(T)@PBE0 calculation still deviates significantly from the high-level references and Δ UKS/PBE0, which is surprising in light of the great performance of Δ UKS/PBE0 itself. To resolve this residual disagreement, it is necessary to adapt the formally wrong $\langle S^2 \rangle$ expectation value of the open-shell singlet (1 instead of 0) with the Yamaguchi correction. This yields the pale dashed red line in Figure 4a, which is finally in reasonable agreement with the other highly correlated methods and Δ UKS/PBE0 for negative and positive ΔE_{ST} . It bears pointing out that the usefulness of the Yamaguchi correction for these coupled-cluster calcula-

tions is in contrast to its impact on Δ UKS/PBE0 itself (see SI), where it disrupts the previously discussed beneficial error cancellation.

To ultimately eliminate any issues resulting from spin-contaminated references, let us consider the ST gaps obtained with the properly spin-adapted two-determinant state-specific coupled cluster, Mk-MR-CCSD(T)@ $\langle\uparrow\downarrow\rangle \pm \langle\downarrow\uparrow\rangle$. Notably, this method predicts slightly more negative ST-gaps than the TBE (MD -0.02 eV, cf. Table I and Figure 3b) and distinctly more negative ST-gaps than the Yamaguchi-corrected Δ CCSD(T)@PBE0. We attribute this disparity to the rudimentary nature of the Yamaguchi spin-correction, lacking the necessary optimization and subsequent stabilization of the spin-pure S_1 state, and the previously discussed high sensitivity of the ST gap to the description of dynamical correlation (large impact of the (T) correction) when using spin-contaminated references. Consequently, even though relative errors between the methods are comparably small (below 0.2 eV between Δ CCSD(T)@PBE0, Mk-MR-CCSD(T), and the TBE), the lack of spin-adaptation precludes the use of Δ CCSD(T)@PBE0 for generating benchmark-quality reference values for ΔE_{ST} . Instead, one should either use spin-adapted Δ approaches, like Mk-MR-CC, or excitation-based methods like EOM-CC. In this context, we want to point out another advantage of the Mk-MR-CC approach over excitation-based methods: Because no substitutions are required to generate the excited state from the reference ground state, the state-specific Mk-MR-CC approach includes more correlation for the singlet and triplet excited states than excitation-based CC methods. This becomes evident from the impact of the (T) correction on the gaps, which is virtually negligible in Mk-MR-CCSD(T) (see Figure S9 in the SI), while triples have a substantial influence in EOM-CCSDT.⁴⁷ Also regarding the basis set, we find the Mk-MR-CC calculations to be essentially converged at a def2-TZVP level, as evident from the negligible effects of using def2-TZVPP (1 meV) or def2-TZVPD (3 meV) on the gap of heptazine (see Table S1 in the SI). This is in contrast to the reported large basis-set effects of Dreuw and Hoffmann.⁴⁸

After extensive discussion of the small and structurally related INVEST15 set, we finally put the robustness of the Δ UKS/PBE0 approach to the test. To this end, we compiled the NAH159 benchmark, which contains structurally diverse systems not included in INVEST15. Further, we want to simulate the conditions of high-throughput screenings, meaning we use the much smaller def2-SVP basis set and avoid any molecule-specific parameters or manual guidance. In other words, we apply the approach in a black-box fashion. This brings up one shortcoming of state-specific excited state methods like Δ DFT: It is not known which occupied and virtual orbitals contribute to the lowest

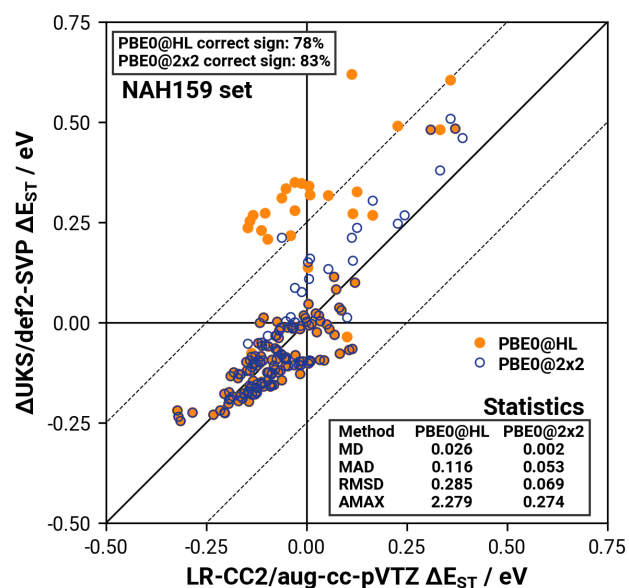


Figure 5. Correlation plot for the vertical singlet-triplet energy gap calculated by Δ PBE0/def2-SVP and LR-CC2/aug-cc-pVTZ for the 159 molecules of the NAH159 benchmark set, for the PBE0@HL only the HOMO–LUMO excitation was modeled and for PBE0@2x2 all excitations between HOMO, HOMO-1, LUMO and LUMO+1 were considered to find the lowest singlet and triplet, dashed lines indicate deviations from reference of ± 0.25 eV, all values in eV.

singlet and triplet excited states. Accordingly, just using the HOMO–LUMO transition may lead to wrong gaps, which is the case in about 10 of 159 molecules for this set. However, due to the low computational cost of UKS calculations, we can mitigate the issue in a similar way to using a larger active space in a CAS-SCF calculation: We consider all singlet and triplet states possible in a 2×2 orbital window, that is, transitions from HOMO-1 or HOMO to LUMO or LUMO+1 and converge them with default settings. After convergence, we calculate gaps between the lowest excited states resulting from this protocol. Exploratory calculations in which we further increased the orbital window did not improve the results for NAH159. However, this might differ for other sets including larger molecules, where this protocol can easily be adapted.

The gaps obtained with this approach, termed PBE0 2×2 as well as with the exclusive HOMO–LUMO guess are plotted against the LR-CC2/aug-cc-pVTZ references in Figure 5. Inspection shows a good correlation with no significant outliers for the 2×2 protocol. Further evaluation of the data confirms that in 83.0% of all cases (77.4% if only the HOMO–LUMO transition is considered), the sign of the gap is correctly predicted. The percentage of molecules with a negative

gap according to LR-CC2 but a positive gap according to Δ UKS/PBE0 (false negatives) is only 7.5% (11.3% if only the HOMO–LUMO transition is considered). The percentage of molecules with a positive gap according to LR-CC2 but a negative gap according to Δ UKS/PBE0 (false positives) is only 9.4% (10.7% if only the HOMO–LUMO transition is considered). The overall MAD is 0.053 eV (0.116 eV if only the HOMO–LUMO transition is considered), and thus only slightly larger than for the much smaller and structurally less diverse INVEST15 set. This illustrates the usefulness of the 2×2 approach, which is further corroborated by the improvement in the Pearson correlation coefficient, which increases from 0.44 for the HOMO–LUMO approach to 0.87 for the 2×2 approach.

For completeness, we also report the performance of other methods that performed well on the smaller INVEST15 benchmark. Using the same 2×2 approach, the r^2 SCAN functional performs slightly worse than PBE0, achieving an MAD of 0.063 eV, a Pearson coefficient of 0.7, and 80% correctly predicted gap signs. To our surprise, even TDA-DFT/PBE0 with the gaps shifted by 0.4 eV (*vide supra*) works surprisingly well, yielding an MAD of only 0.060 eV, with the same percentage of correctly predicted gap signs, 83.0%, as for Δ UKS/PBE0@ 2×2 , while the computational cost is comparable. Plots and further statistical data for these approaches can be found in the SI.

During the final stages of the preparation of this manuscript, Kusakabe and coworkers reported an experimental measurement of an ST-gap for a molecule derived from #4 (termed 5AP-N(C12)₂) from the INVEST15 set and closely related to the molecules of the NAH159 set.²⁷ This second experimental conformation of molecular INVEST provided an ST gap of -0.032 eV to -0.043 eV, which agrees reasonably well with the Δ UKS/PBE0/def2-SVP result of -0.02 eV (and furthermore with the SCS-CC2 calculations reported in the original manuscript).

In summary, the results for NAH159 demonstrate that a similar accuracy as in the INVEST15 benchmark can be achieved without human intervention at a tiny fraction of the computation cost of the LR-CC2 calculations. For example, the total walltime for all eight singlet and triplet states for the biggest molecule tested (46 atoms, 428 basis functions with def2-SVP) takes roughly 20 minutes on a quad-core Intel Xeon E3-1270 v5 @ 3.6 GHz compute node. The respective LR-CC2/aug-cc-pVTZ calculation including 10 singlet and 10 triplets (required to find the lowest states reliably) runs over 83 hours on the same machine, which is about 250 times slower than Δ UKS. It should be noted that employing LR-CC2 with a smaller basis set reduces the advantage of Δ UKS to a factor of 80 and 5 for cc-pVTZ and cc-pVDZ, respectively. However, this will also impact the accuracy, and at least the small cc-pVDZ would

introduce substantial errors. Moreover, similar performance optimizations can be done for the Δ UKS calculations, e.g., by using density-fitting for coulomb and exchange integrals (which is not implemented in Q-Chem), particularly for r^2 SCAN, or switching to the even smaller 6-31G basis set, which more than halves the wall time without affecting the accuracy too much (see Figure S10 in SI).

Summary and Conclusion — This study explored the accurate prediction of inverted singlet-triplet energy gaps (INVEST), focusing on efficient yet robust alternatives to computationally demanding wavefunction-based approaches. The main finding is that the intriguingly simple and computationally cheap Δ UKS/PBE0 approach shows a surprisingly robust performance (MAD 0.046 eV for INVEST15, 0.053 eV for NAH159) comparable to much more demanding wavefunction-based approaches. Further results using methods ranging from standard density functional theory (DFT) to more sophisticated wavefunction-based approaches and combinations thereof were used to rationalize the performance of Δ UKS/PBE0, tracing it back to a robust spin-polarization-based error-cancellation.

Further key findings from the study include:

- **Role of Fock-Exchange:** Including exact Fock exchange in Δ UKS calculations (i.e., using hybrid functionals) is critical. The study demonstrates that a moderate amount of FX, as in PBE0 or tuned range-separated hybrids, provides the most reliable predictions. This is due to the effective handling of dynamic spin-polarization, which depends on the balance between spin contamination and dynamic correlation and is required for accurate gap predictions. An exception appears to be the r^2 SCAN functional, which despite its mGGA nature predicts gaps with the same accuracy as PBE0 (MAD 0.053 eV for INVEST15, 0.061 eV for NAH159) except for a few outliers. mGGA functionals are interesting as they can fully exploit the density-fitting approximation, allowing for even faster calculations.
- **State-Specific Post-SCF Correlation Methods:** Advanced correlation methods such as CCSD(T) correct the spin contamination observed in simpler methods and improve the reliability of the predictions, though they require careful consideration of the reference wavefunction and spin state. An elegant solution is provided to use a spin-adapted two-determinant reference for the singlet, as evident from the superior performance of state-specific Mk-MR-CC, which is converged at the CCSD level in a triple-zeta basis set, where other excitation-based CC methods required at least perturbative triples for the same accuracy.

- **High-Throughput Applications:** In a test application of Δ UKS/PBE0 to a large and structurally diverse benchmark, the sign of the ST gap was predicted in agreement with LR-CC2 in 83% of all cases, with less than 10% false positive and less than 8% false negatives, and only slightly worse error-statistics than for the smaller INVEST15 benchmark. For this, we considered all excitation from HOMO and HOMO-1 to LUMO and LUMO+1 to avoid issues with the state-specific method converging on higher-lying states. Since Δ UKS/PBE0 dramatically reduces the computational cost by two orders of magnitude compared to the wavefunction-based LR-CC2 reference (or the number of required LR-CC2 calculations if Δ UKS/PBE0 is used in a pre-screening), the reported method is a promising candidate for the high-throughput computational exploration of new INVEST materials.

Overall, this research sheds light on the effectiveness of hybrid density functionals and modern mGGA functionals in capturing the essential physics of singlet-triplet gap inversion in INVEST emitters. It also highlights the potential of Δ UKS in providing a computationally efficient alternative to more demanding methods, thus paving the way for rapid and reliable materials discovery in the field of organic electronics.

Acknowledgment — This project has been funded with support from the RTG-2591 "TIDE - Template-designed Organic Electronics". T.F. is most grateful to the "Fonds der Chemischen Industrie (FCI)" for financial support under a Kekulé scholarship. The authors gratefully acknowledge the granted access to the Marvin cluster hosted by the University of Bonn.

Supporting Information Available: Detailed computational settings and workflows, singlet and triplet excitation energies for TDA-DFT results, singlet and triplet excitation energies for Δ UKS results, spin-expectation values for all singlet and triplet states for Δ UKS, the effect of solvation environment (modeled by a PCM) on the singlet-triplet gap calculated by Δ UKS, basis set convergence of the singlet-triplet gap results for Δ UKS and Δ CC methods, comparison of different WFT approaches for the singlet-triplet gap calculated by Δ CC, comparison of different MR-Mk-CC approaches for the calculation of the singlet-triplet gap, choice of the theoretical reference, further NAH159 set Δ UKS results, formulas for statistical measures, libre-office spreadsheet of all relevant data points, geometries of all studied molecules in .xyz-file format (.zip-archive)

Conflicts of interest — There are no conflicts to declare.

REFERENCES

- (1) de Silva, P. Inverted singlet–triplet gaps and their relevance to thermally activated delayed fluorescence. *The Journal of Physical Chemistry Letters* **2019**, *10*, 5674–5679.
- (2) Ehrmaier, J.; Rabe, E. J.; Pristash, S. R.; Corp, K. L.; Schlenker, C. W.; Sobolewski, A. L.; Domcke, W. Singlet–triplet inversion in heptazine and in polymeric carbon nitrides. *The Journal of Physical Chemistry A* **2019**, *123*, 8099–8108.
- (3) Dinkelbach, F.; Bracker, M.; Kleinschmidt, M.; Mariani, C. M. Large inverted singlet–triplet energy gaps are not always favorable for triplet harvesting: Vibronic coupling drives the (reverse) intersystem crossing in heptazine derivatives. *The Journal of Physical Chemistry A* **2021**, *125*, 10044–10051.
- (4) Pollice, R.; Friederich, P.; Lavigne, C.; dos Passos Gomes, G.; Aspuru-Guzik, A. Organic molecules with inverted gaps between first excited singlet and triplet states and appreciable fluorescence rates. *Matter* **2021**, *4*, 1654–1682.
- (5) Sobolewski, A. L.; Domcke, W. Are heptazine-based organic light-emitting diode chromophores thermally activated delayed fluorescence or inverted singlet–triplet systems? *The Journal of Physical Chemistry Letters* **2021**, *12*, 6852–6860.
- (6) Sanz-Rodrigo, J.; Ricci, G.; Olivier, Y.; Sancho-García, J.-C. Negative singlet–triplet excitation energy gap in triangle-shaped molecular emitters for efficient triplet harvesting. *The Journal of Physical Chemistry A* **2021**, *125*, 513–522.
- (7) Ricci, G.; Sancho-García, J.-C.; Olivier, Y. Establishing design strategies for emissive materials with an inverted singlet–triplet energy gap (INVEST): a computational perspective on how symmetry rules the interplay between triplet harvesting and light emission. *Journal of Materials Chemistry C* **2022**, *10*, 12680–12698.
- (8) Tučková, L.; Straka, M.; Valiev, R. R.; Sundholm, D. On the origin of the inverted singlet–triplet gap of the 5th generation light-emitting molecules. *Physical Chemistry Chemical Physics* **2022**, *24*, 18713–18721.
- (9) Ghosh, S.; Bhattacharyya, K. Origin of the failure of density functional theories in predicting inverted singlet–triplet gaps. *The Journal of Physical Chemistry A* **2022**, *126*, 1378–1385.
- (10) Li, J.; Li, Z.; Liu, H.; Gong, H.; Zhang, J.; Yao, Y.; Guo, Q. Organic molecules with inverted singlet–triplet gaps. *Frontiers in Chemistry* **2022**, *10*, 999856.
- (11) Aizawa, N.; Pu, Y.-J.; Harabuchi, Y.; Nihonyanagi, A.; Ibuka, R.; Inuzuka, H.; Dhara, B.; Koyama, Y.; Nakayama, K.-i.; Maeda, S.; others Delayed fluorescence from inverted singlet and triplet excited states. *Nature* **2022**, *609*, 502–506.
- (12) Terence Blaskovits, J.; Garner, M. H.; Corminboeuf, C. Symmetry-Induced Singlet-Triplet Inversions in Non-Alternant Hydrocarbons. *Angewandte Chemie International Edition* **2023**, *62*, e202218156.
- (13) Mitschke, U.; Bäuerle, P. The electroluminescence of organic materials. *Journal of Materials Chemistry* **2000**, *10*, 1471–1507.
- (14) Zhang, Q.; Li, J.; Shizu, K.; Huang, S.; Hirata, S.; Miyazaki, H.; Adachi, C. Design of efficient thermally activated delayed fluorescence materials for pure blue organic light emitting diodes. *Journal of the American Chemical Society* **2012**, *134*, 14706–14709.
- (15) Tao, Y.; Yuan, K.; Chen, T.; Xu, P.; Li, H.; Chen, R.; Zheng, C.; Zhang, L.; Huang, W. Thermally activated delayed fluorescence materials towards the breakthrough of organoelectronics. *Advanced materials* **2014**, *26*, 7931–7958.
- (16) Hirata, S.; Sakai, Y.; Masui, K.; Tanaka, H.; Lee, S. Y.; Nomura, H.; Nakamura, N.; Yasumatsu, M.; Nakanotani, H.; Zhang, Q.; others Highly efficient blue electroluminescence based on thermally activated delayed fluorescence. *Nature materials* **2015**, *14*, 330–336.
- (17) Dias, F. B.; Penfold, T. J.; Monkman, A. P. Photophysics of thermally activated delayed fluorescence molecules. *Methods and applications in fluorescence* **2017**, *5*, 012001.
- (18) Yang, Z.; Mao, Z.; Xie, Z.; Zhang, Y.; Liu, S.; Zhao, J.; Xu, J.; Chi, Z.; Aldred, M. P. Recent advances in organic thermally activated delayed fluorescence materials. *Chemical Society Reviews* **2017**, *46*, 915–1016.
- (19) Wong, M. Y.; Zysman-Colman, E. Purely organic thermally activated delayed fluorescence materials for organic light-emitting diodes. *Advanced Materials* **2017**, *29*, 1605444.
- (20) Liu, Y.; Li, C.; Ren, Z.; Yan, S.; Bryce, M. R. All-organic thermally activated delayed fluorescence materials for organic light-emitting diodes. *Nature Reviews Materials* **2018**, *3*, 1–20.
- (21) Mewes, J.-M. Modeling TADF in organic emitters requires a careful consideration of the environment and going beyond the Franck–Condon approximation. *Physical Chemistry Chemical Physics* **2018**, *20*, 12454–12469.
- (22) Teng, J.-M.; Wang, Y.-F.; Chen, C.-F. Recent progress of narrowband TADF emitters and their applications in OLEDs. *Journal of Materials Chemistry C* **2020**, *8*, 11340–11353.
- (23) Madayanad Suresh, S.; Hall, D.; Beljonne, D.; Olivier, Y.; Zysman-Colman, E. Multiresonant thermally activated delayed fluorescence emitters based on heteroatom-doped nanographenes: recent advances and prospects for organic light-emitting diodes. *Advanced Functional Materials* **2020**, *30*, 1908677.
- (24) Naveen, K. R.; Palanisamy, P.; Chae, M. Y.; Kwon, J. H. Multiresonant TADF materials: triggering the reverse intersystem crossing to alleviate the efficiency roll-off in OLEDs. *Chemical Communications* **2023**, *59*, 3685–3702.
- (25) Seifermann, S. Organic molecules for optoelectronic devices. U.S. Patent US11545632B2. January 3, 2023.
- (26) Actis, A.; Melchionna, M.; Filippini, G.; Fornasiero, P.; Prato, M.; Chiesa, M.; Salvadori, E. Singlet-Triplet Energy Inversion in Carbon Nitride Photocatalysts. *Angewandte Chemie International Edition* **2023**, *62*, e202313540.
- (27) Kusakabe, Y.; SHIZU, K.; Tanaka, H.; Tanaka, K.;

- Kaji, H. An inverted singlet-triplet excited state in a pentaazaphenalene derivative (5AP-N (C12) 2). *Applied Physics Express* **2024**,
- (28) Runge, E.; Gross, E. K. Density-functional theory for time-dependent systems. *Physical review letters* **1984**, *52*, 997.
- (29) Hirata, S.; Head-Gordon, M. Time-dependent density functional theory within the Tamm–Dancoff approximation. *Chemical Physics Letters* **1999**, *314*, 291–299.
- (30) Froitzheim, T.; Grimme, S.; Mewes, J.-M. Either accurate singlet–triplet gaps or excited-state structures: Testing and understanding the performance of td-dft for tadf emitters. *Journal of Chemical Theory and Computation* **2022**, *18*, 7702–7713.
- (31) Froitzheim, T.; Kunze, L.; Grimme, S.; Herbert, J.; Mewes, J.-M. Benchmarking Charge-Transfer Excited States in TADF Emitters: Δ DFT outperforms TD-DFT for Emission Energies. *chemrxiv preprint 10.26434/chemrxiv-2024-10550* **2024**,
- (32) Hall, D.; Sancho-García, J. C.; Pershin, A.; Ricci, G.; Beljonne, D.; Zysman-Colman, E.; Olivier, Y. Modeling of multiresonant thermally activated delayed fluorescence emitters – properly accounting for electron correlation is key! *Journal of Chemical Theory and Computation* **2022**, *18*, 4903–4918.
- (33) Kimber, P.; Plasser, F. Toward an understanding of electronic excitation energies beyond the molecular orbital picture. *Physical Chemistry Chemical Physics* **2020**, *22*, 6058–6080.
- (34) Drwal, D.; Matousek, M.; Golub, P.; Tucholska, A.; Hapka, M.; Brabec, J.; Veis, L.; Pernal, K. Role of Spin Polarization and Dynamic Correlation in Singlet–Triplet Gap Inversion of Heptazine Derivatives. *Journal of Chemical Theory and Computation* **2023**, *19*, 7606–7616.
- (35) Kollmar, H.; Staemmler, V. Violation of Hund’s rule by spin polarization in molecules. *Theoretica chimica acta* **1978**, *48*, 223–239.
- (36) Ricci, G.; San-Fabian, E.; Olivier, Y.; Sancho-García, J.-C. Singlet-triplet excited-state inversion in heptazine and related molecules: assessment of TD-DFT and ab initio methods. *ChemPhysChem* **2021**, *22*, 553–560.
- (37) Won, T.; Nakayama, K.-i.; Aizawa, N. Inverted singlet–triplet emitters for organic light-emitting diodes. *Chemical Physics Reviews* **2023**, *4*.
- (38) Christiansen, O.; Koch, H.; Jørgensen, P. The second-order approximate coupled cluster singles and doubles model CC2. *Chemical Physics Letters* **1995**, *243*, 409–418.
- (39) Schirmer, J. Beyond the random-phase approximation: A new approximation scheme for the polarization propagator. *Physical Review A* **1982**, *26*, 2395.
- (40) Trofimov, A.; Schirmer, J. An efficient polarization propagator approach to valence electron excitation spectra. *Journal of Physics B: Atomic, Molecular and Optical Physics* **1995**, *28*, 2299.
- (41) Grimme, S. Improved second-order Møller–Plesset perturbation theory by separate scaling of parallel- and antiparallel-spin pair correlation energies. *The Journal of chemical physics* **2003**, *118*, 9095–9102.
- (42) Hellweg, A.; Grün, S. A.; Hättig, C. Benchmarking the performance of spin-component scaled CC2 in ground and electronically excited states. *Physical Chemistry Chemical Physics* **2008**, *10*, 4119–4127.
- (43) Roos, B. O.; Taylor, P. R.; Sigbahn, P. E. A complete active space SCF method (CASSCF) using a density matrix formulated super-CI approach. *Chemical Physics* **1980**, *48*, 157–173.
- (44) Angeli, C.; Cimiraglia, R.; Evangelisti, S.; Leininger, T.; Malrieu, J.-P. Introduction of n-electron valence states for multireference perturbation theory. *The Journal of Chemical Physics* **2001**, *114*, 10252–10264.
- (45) Andersson, K.; Malmqvist, P. A.; Roos, B. O.; Sadlej, A. J.; Wolinski, K. Second-order perturbation theory with a CASSCF reference function. *Journal of Physical Chemistry* **1990**, *94*, 5483–5488.
- (46) Andersson, K.; Malmqvist, P.-Å.; Roos, B. O. Second-order perturbation theory with a complete active space self-consistent field reference function. *The Journal of chemical physics* **1992**, *96*, 1218–1226.
- (47) Loos, P.-F.; Lipparini, F.; Jacquemin, D. Heptazine, Cyclazine, and Related Compounds: Chemically-Accurate Estimates of the Inverted Singlet–Triplet Gap. *The Journal of Physical Chemistry Letters* **2023**, *14*, 11069–11075.
- (48) Dreuw, A.; Hoffmann, M. The inverted singlet–triplet gap: a vanishing myth? *Frontiers in Chemistry* **2023**, *11*.
- (49) Raghavachari, K.; Trucks, G. W.; Pople, J. A.; Head-Gordon, M. A fifth-order perturbation comparison of electron correlation theories. *Chemical Physics Letters* **1989**, *157*, 479–483.
- (50) Mahapatra, U. S.; Datta, B.; Mukherjee, D. A size-consistent state-specific multireference coupled cluster theory: Formal developments and molecular applications. *The Journal of chemical physics* **1999**, *110*, 6171–6188.
- (51) Mahapatra, U. S.; Datta, B.; Mukherjee, D. Development of a size-consistent state-specific multireference perturbation theory with relaxed model-space coefficients. *Chemical physics letters* **1999**, *299*, 42–50.
- (52) Koch, H.; Christiansen, O.; Sanchez de Merás, A. M.; Helgaker, T.; others The CC3 model: An iterative coupled cluster approach including connected triples. *The Journal of chemical physics* **1997**, *106*, 1808–1818.
- (53) Kucharski, S. A.; Włoch, M.; Musiał, M.; Bartlett, R. J. Coupled-cluster theory for excited electronic states: The full equation-of-motion coupled-cluster single, double, and triple excitation method. *The Journal of Chemical Physics* **2001**, *115*, 8263–8266.
- (54) Jorner, K.; Pollice, R.; Lavigne, C.; Aspuru-Guzik, A. Ultrafast computational screening of molecules with inverted singlet-triplet energy gaps using the Pariser-Parr-Pople semi-empirical quantum chemistry method. **2024**,
- (55) Gilbert, A. T.; Besley, N. A.; Gill, P. M. Self-consistent field calculations of excited states using the

- maximum overlap method (MOM). *The Journal of Physical Chemistry A* **2008**, *112*, 13164–13171.
- (56) Barca, G. M.; Gilbert, A. T.; Gill, P. M. Simple models for difficult electronic excitations. *Journal of chemical theory and computation* **2018**, *14*, 1501–1509.
- (57) Frank, I.; Hutter, J.; Marx, D.; Parrinello, M. Molecular dynamics in low-spin excited states. *The Journal of chemical physics* **1998**, *108*, 4060–4069.
- (58) Filatov, M.; Shaik, S. A spin-restricted ensemble-referenced Kohn–Sham method and its application to diradicaloid situations. *Chemical physics letters* **1999**, *304*, 429–437.
- (59) Kowalczyk, T.; Tsuchimochi, T.; Chen, P.-T.; Top, L.; Van Voorhis, T. Excitation energies and Stokes shifts from a restricted open-shell Kohn–Sham approach. *The Journal of chemical physics* **2013**, *138*.
- (60) Garner, M. H.; Blaskovits, J. T.; Corminboeuf, C. Enhanced inverted singlet–triplet gaps in azaphenalenenes and non-alternant hydrocarbons. *Chemical Communications* **2024**.
- (61) Balková, A.; Bartlett, R. J. Coupled-cluster method for open-shell singlet states. *Chemical physics letters* **1992**, *193*, 364–372.
- (62) Lutz, J. J.; Nooijen, M.; Perera, A.; Bartlett, R. J. Reference dependence of the two-determinant coupled-cluster method for triplet and open-shell singlet states of biradical molecules. *The Journal of Chemical Physics* **2018**, *148*.
- (63) Purvis III, G. D.; Bartlett, R. J. A full coupled-cluster singles and doubles model: The inclusion of disconnected triples. *The Journal of Chemical Physics* **1982**, *76*, 1910–1918.
- (64) Yamaguchi, K.; Jensen, F.; Dorigo, A.; Houk, K. A spin correction procedure for unrestricted Hartree–Fock and Møller–Plesset wavefunctions for singlet diradicals and polyradicals. *Chemical physics letters* **1988**, *149*, 537–542.
- (65) Bhaskaran-Nair, K.; Brabec, J.; Aprà, E.; van Dam, H. J.; Pittner, J.; Kowalski, K. Implementation of the multireference Brillouin–Wigner and Mukherjee’s coupled cluster methods with non-iterative triple excitations utilizing reference-level parallelism. *The Journal of Chemical Physics* **2012**, *137*.
- (66) Damour, Y.; Scemama, A.; Jacquemin, D.; Kossowski, F.; Loos, P.-F. State-Specific Coupled-Cluster Methods for Excited States. *arXiv preprint arXiv:2401.05048* **2024**.
- (67) Epifanovsky, E.; Gilbert, A. T.; Feng, X.; Lee, J.; Mao, Y.; Mardirossian, N.; Pokhilko, P.; White, A. F.; Coons, M. P.; Dempwolff, A. L.; others Software for the frontiers of quantum chemistry: An overview of developments in the Q-Chem 5 package. *The Journal of chemical physics* **2021**, *155*.
- (68) Neese, F.; Wennmohs, F.; Becker, U.; Riplinger, C. The ORCA quantum chemistry program package. *The Journal of chemical physics* **2020**, *152*.
- (69) Hohenberg, P.; Kohn, W. Inhomogeneous electron gas. *Physical review* **1964**, *136*, B864.
- (70) Kohn, W.; Sham, L. J. Self-consistent equations including exchange and correlation effects. *Physical review* **1965**, *140*, A1133.
- (71) Kállay, M.; Nagy, P. R.; Mester, D.; Rolik, Z.; Samu, G.; Csontos, J.; Csóka, J.; Szabó, P. B.; Gyevi-Nagy, L.; Hégyel, B.; others The MRCC program system: Accurate quantum chemistry from water to proteins. *The Journal of chemical physics* **2020**, *152*.
- (72) Apra, E.; Bylaska, E. J.; De Jong, W. A.; Govind, N.; Kowalski, K.; Straatsma, T. P.; Valiev, M.; van Dam, H. J.; Alexeev, Y.; Anchell, J.; others NWChem: Past, present, and future. *The Journal of chemical physics* **2020**, *152*.
- (73) Mejia-Rodriguez, D.; Aprà, E.; Autschbach, J.; Bauman, N. P.; Bylaska, E. J.; Govind, N.; Hammond, J. R.; Kowalski, K.; Kunitsa, A.; Panyala, A.; others NWChem: Recent and Ongoing Developments. *Journal of Chemical Theory and Computation* **2023**, *19*, 7077–7096.
- (74) Hirata, S. Tensor contraction engine: Abstraction and automated parallel implementation of configuration-interaction, coupled-cluster, and many-body perturbation theories. *The Journal of Physical Chemistry A* **2003**, *107*, 9887–9897.
- (75) Aidas, K.; Angeli, C.; Bak, K. L.; Bakken, V.; Bast, R.; Boman, L.; Christiansen, O.; Cimiraglia, R.; Coriani, S.; Dahle, P.; others The Dalton quantum chemistry program system. *Wiley Interdisciplinary Reviews: Computational Molecular Science* **2014**, *4*, 269–284.
- (76) Dalton, a Molecular Electronic Structure Program, Release Dalton2020.1 (2022), see <http://daltonprogram.org>.
- (77) Brandenburg, J. G.; Bannwarth, C.; Hansen, A.; Grimme, S. B97-3c: A revised low-cost variant of the B97-D density functional method. *The Journal of chemical physics* **2018**, *148*.
- (78) Weigend, F.; Ahlrichs, R. Balanced basis sets of split valence, triple zeta valence and quadruple zeta valence quality for H to Rn: Design and assessment of accuracy. *Physical Chemistry Chemical Physics* **2005**, *7*, 3297–3305.
- (79) Weigend, F. Accurate Coulomb-fitting basis sets for H to Rn. *Physical chemistry chemical physics* **2006**, *8*, 1057–1065.
- (80) Dunning Jr, T. H. Gaussian basis sets for use in correlated molecular calculations. I. The atoms boron through neon and hydrogen. *The Journal of chemical physics* **1989**, *90*, 1007–1023.
- (81) Woon, D. E.; Dunning Jr, T. H. Gaussian basis sets for use in correlated molecular calculations. III. The atoms aluminum through argon. *The Journal of chemical physics* **1993**, *98*, 1358–1371.
- (82) Kendall, R. A.; Dunning Jr, T. H.; Harrison, R. J. Electron affinities of the first-row atoms revisited. Systematic basis sets and wave functions. *The Journal of chemical physics* **1992**, *96*, 6796–6806.
- (83) Chai, J.-D.; Head-Gordon, M. Long-range corrected hybrid density functionals with damped atom–atom dispersion corrections. *Physical Chemistry Chemical Physics* **2008**, *10*, 6615–6620.
- (84) Mester, D.; Nagy, P. R.; Kállay, M. Reduced-cost linear-response CC2 method based on natural orbitals and natural auxiliary functions. *The Journal of Chem-*

- ical Physics* **2017**, *146*.
- (85) Perdew, J. P.; Burke, K.; Ernzerhof, M. Generalized gradient approximation made simple. *Physical review letters* **1996**, *77*, 3865.
- (86) Burke, K.; Ernzerhof, M.; Perdew, J. P. The adiabatic connection method: a non-empirical hybrid. *Chemical Physics Letters* **1997**, *265*, 115–120.
- (87) Adamo, C.; Barone, V. Toward reliable density functional methods without adjustable parameters: The PBE0 model. *The Journal of chemical physics* **1999**, *110*, 6158–6170.
- (88) Grimme, S.; Antony, J.; Ehrlich, S.; Krieg, H. A consistent and accurate ab initio parametrization of density functional dispersion correction (DFT-D) for the 94 elements H-Pu. *The Journal of chemical physics* **2010**, *132*.
- (89) Bernard, Y. A.; Shao, Y.; Krylov, A. I. General formulation of spin-flip time-dependent density functional theory using non-collinear kernels: Theory, implementation, and benchmarks. *The Journal of chemical physics* **2012**, *136*.
- (90) Weintraub, E.; Henderson, T. M.; Scuseria, G. E. Long-range-corrected hybrids based on a new model exchange hole. *Journal of Chemical Theory and Computation* **2009**, *5*, 754–762.
- (91) Kunze, L.; Hansen, A.; Grimme, S.; Mewes, J.-M. PCM-ROKS for the Description of Charge-Transfer States in Solution: Singlet–Triplet Gaps with Chemical Accuracy from Open-Shell Kohn–Sham Reaction-Field Calculations. *The Journal of Physical Chemistry Letters* **2021**, *12*, 8470–8480.
- (92) Tozer, D. J.; Handy, N. C. On the determination of excitation energies using density functional theory. *Physical Chemistry Chemical Physics* **2000**, *2*, 2117–2121.
- (93) Elliott, P.; Goldson, S.; Canahui, C.; Maitra, N. T. Perspectives on double-excitations in TDDFT. *Chemical Physics* **2011**, *391*, 110–119.
- (94) Maitra, N. T. Double and charge-transfer excitations in time-dependent density functional theory. *Annual review of physical chemistry* **2022**, *73*, 117–140.
- (95) Do Casal, M. T.; Toldo, J. M.; Barbatti, M.; Plasser, F. Classification of doubly excited molecular electronic states. *Chemical Science* **2023**, *14*, 4012–4026.
- (96) Bursch, M.; Mewes, J.-M.; Hansen, A.; Grimme, S. Best-practice DFT protocols for basic molecular computational chemistry. *Angewandte Chemie International Edition* **2022**, *61*, e202205735.
- (97) Furness, J. W.; Kaplan, A. D.; Ning, J.; Perdew, J. P.; Sun, J. Accurate and numerically efficient r2SCAN meta-generalized gradient approximation. *The journal of physical chemistry letters* **2020**, *11*, 8208–8215.
- (98) Mardirossian, N.; Head-Gordon, M. Mapping the genome of meta-generalized gradient approximation density functionals: The search for B97M-V. *The Journal of chemical physics* **2015**, *142*.
- (99) Spada, R. F.; Franco, M. P.; Nieman, R.; Aquino, A. J.; Shepard, R.; Plasser, F.; Lischka, H. Spin-density calculation via the graphical unitary group approach. *Molecular Physics* **2023**, *121*, e2091049.
- (100) Neugebauer, H.; Vuong, H. T.; Weber, J. L.; Friesner, R. A.; Shee, J.; Hansen, A. Toward Benchmark-Quality Ab Initio Predictions for 3d Transition Metal Electrocatalysts: A Comparison of CCSD (T) and ph-AFQMC. *Journal of Chemical Theory and Computation* **2023**, *19*, 6208–6225.